Cooperative Object Transportation by Multiple Ground and Aerial Vehicles: Modeling and Planning

Conference Paper · May 2018

DOI: 10.1109/ICRA.2018.8460778

2 authors:

Martina Lippi
Università degli Studi di Salerno
3 PUBLICATIONS **1** CITATION
SEE PROFILE

Alessandro Marino
Università degli Studi di Salerno
57 PUBLICATIONS **620** CITATIONS
SEE PROFILE

Cooperative object transportation by multiple ground and aerial vehicles: modeling and planning

Martina Lippi, Alessandro Marino*, *IEEE Senior Member*

***Abstract*— In this paper, the modeling and planning problems of a system composed of multiple ground and aerial robots involved in a transportation task are considered. The ground robots rigidly grasp a load, while the aerial vehicles are attached to the object through non-rigid inextensible cables. The idea behind such a heterogeneous multi-robot system is to benefit of the advantages of both types of robots that might be the precision of ground robots and the high pay-load of multiple aerial vehicles. The overall model of the system is derived and its expression and redundancy are exploited by setting a general constrained optimal planning problem. The problem is herein solved by dynamic programming and simulation results validated the proposed scheme.**

I. INTRODUCTION

The research community has devoted a large effort in the last decade towards aerial service robots and, in particular, to Unmanned Aerial Vehicles (UAVs). Moreover, many authors have focused on the load transportation task by single or more aerial vehicles. The task can be achieved by adopting cooperative aerial manipulators [1] or by using cables attached to the UAVs and the payload [2], [3], where these cables are either rigid [4] or flexible [5]. In the latter case, cables substitute manipulators equipped with grippers, that heavily contribute to saturate the payload of the UAV, while the risk of collisions might be reduced by increasing the extension of cables; however, this comes at the cost of a more complexity of the system model and of the control design, mainly due to the fact that tensions along cables cannot be negative. In [6], the authors consider the case of transporting an unknown load by using a flexible cable and a single UAV (namely a quadrotor) controlled via a fixed-gain nonlinear proportional-derivative adaptive controller. A single quadrotor is also considered in [7] where a non-linear controller is designed based on the differential flatness of the overall system that, remarkably, allows trajectory generation even in the case when the tension in the cable goes to zero. In [8], flatness, controllability and observability properties of a suspended load carried by an UAV are exploited to design a model-based nonlinear controller, whose aim is to track a smooth time-varying trajectory of the load.

In order to prevent oscillations of the load due to cables and also to handle the case of rigid-body loads, the case of multi-UAVs have been widely considered in the literature. Within this framework, the authors in [4] presented a model-based control law for the case of a point mass load connected to multiple UAVs by mass-less links, in which quadrotors maintain a prescribed formation. An arbitrary number of quadrotors is considered which are possibly connected to the load with rigid links and with the possibility of having the UAVs below the load in an inverted pendulum configuration.

Martina Lippi and Alessandro Marino are with University of Salerno, Via Giovanni Paolo II, 132, 84084, Salerno (SA), Italy email: {mlippi,almarino}@unisa.it

*Authors are in alphabetical order

The work in [7] is exploited in [9] to design a geometric feedback control to track a reference trajectory for the load, the yaw angle of each quadrotor, and the orientation of cables.

The connection between the cooperative aerial transportation of an object using a team of quadrotors and reconfigurable cable-driven parallel robots is remarked in [5]. A rigid body load is considered and a closed-loop inverse dynamics control is design based on a kinematic and dynamic model of the whole system. Moreover, in the case the number of links is greater than the number of the degrees of freedom of the object to control, the tension distribution is not unique. This feature is exploited by the authors to locally optimize the tension distribution along the cables.

Finally, the authors in [10] resort to a robust Model Predictive Control (MPC) technique for tracking a time-varying reference trajectory for the load connected by flexible cables to quadrotors. This trajectory is obtained by solving a constrained optimization problem in which UAVs are assumed to be in formation.

There are also a few recent papers dealing with the cooperation of UAVs and Unmanned Ground Vehicles (UGVs) that are dynamically interconnected. For example, in [11] an UAV and an UGV cooperate to manipulate a rigid object under actuator saturations. The UGV is in charge of deploying the object to a certain position and a saturated PD control law is used to this purpose, while the UAV is in charge of adjusting the object's orientation and is governed by a cascade controller. Another example of cooperation between UAVs and UGVs is represented by [12]. A different problem is addressed in that work, since a system composed by a single UAV connected to multiple UGVs by cables is tackled and no object to transport is present. UGVs are considered as mobile actuators that, through the cables, are able to properly modify the position dynamics of the UAV and improve the controllability of the aerial vehicle and its capability to react to external disturbances. Finally, in [13], a ground manipulator and a team of aerial robots are used to cooperatively manipulate a load. The idea is to have the manipulator exploit its higher payload to handle the object while letting the UAVs to perform only small adjustments. A nonlinear control scheme in the case of several sources of uncertainties and constraints is presented.

The aim of this paper is to lay the foundation of a general framework for the cooperative transportation of a rigid load by multiple UAVs and UGVs. Any number of ground and aerial vehicles is allowed, and the load is connected to UAVs by cables, while manipulators rigidly grasp the object. The model of the overall system is devised, and its expression and the system redundancy are exploited to set a general constraint optimal planning problem where any type of constraints and performance index can be considered. Examples of constraints are the minimum and maximum tensions along

the cables or the safety distance between aerial vehicles, while the performance index might be chosen in such a way to optimize the distribution of the load among ground and aerial vehicles and/or the formation assumed by the latter.

The remainder of the paper is organized as follows. In Section II, the system, the mathematical formulation and the problem setting are presented in detail. In Section III, a solution to the problem is proposed and discussed, while its effectiveness is shown in Section IV. Finally, conclusions and recommendations for future work are drawn in Section V.

II. Mathematical Background

Let us consider the system in Figure 1, where N_a aerial vehicles and N_g ground mobile manipulators transport a rigid object. It is assumed that the aerial vehicles are connected to the load through inextensible, weightless cables.

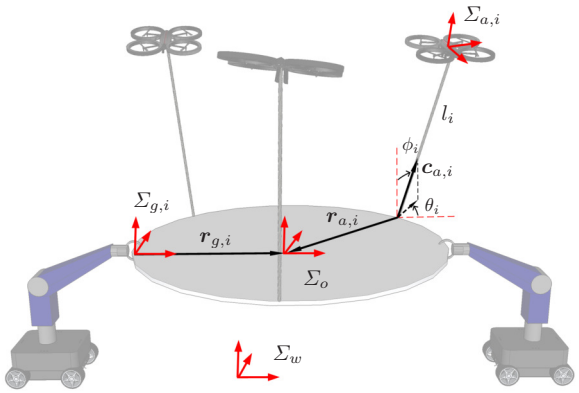

Fig. 1. Representation of the considered multi-robot system composed by both ground and aerial vehicles.

In the figure

- Σ_w is the world reference frame;
- Σ_o is the object reference frame whose origin and orientation with respect to Σ_w are $\boldsymbol{p}_o \in \mathbb{R}^3$ and $\boldsymbol{R}_o \in \mathbb{R}^{3\times3}$, respectively;
- $\Sigma_{g,i}$ is the reference frame attached to the end-effector of the ith ground robot, whose origin and orientation with respect to Σ_w are $\boldsymbol{p}_{g,i} \in \mathbb{R}^3$ and $\boldsymbol{R}_{g,i} \in \mathbb{R}^{3\times3}$, respectively;
- $\Sigma_{a,i}$ is the reference frame of the ith aerial robot, whose origin and orientation with respect to Σ_w are $\boldsymbol{p}_{a,i} \in \mathbb{R}^3$ and $\boldsymbol{R}_{a,i} \in \mathbb{R}^{3\times3}$, respectively. Moreover, $\boldsymbol{p}_{a,i}$ coincides with the center of mass of the aerial robot;
- $\boldsymbol{r}_{g,i} \in \mathbb{R}^3$ is the vector pointing from the contact point of the ith ground-robot end-effector to the object center of mass, expressed in Σ_w;
- $\boldsymbol{r}_{a,i} \in \mathbb{R}^3$ is the vector pointing from the attach point on the object of the ith quadrotor's cable to the object center of mass, expressed in Σ_w;
- $\boldsymbol{c}_{a,i} \in \mathbb{R}^3$ is the unit vector pointing from the attach point on the object of the ith cable to $\boldsymbol{p}_{a,i}$ expressed in the frame Σ_w;
- $l_i \in \mathbb{R}^+$ is the length of the ith cable.

A. Manipulators' dynamics

Let us consider the following assumption.

Assumption 1. *It is assumed that each ground robot rigidly grasps the object and that the end-effector is fully actuated and equipped by a force sensor.*

Such an assumption is realistic for many commercially available platforms and allows to apply a nonlinear dynamic approach to control ground robots, that ultimately leads to the following linear dynamic behavior assumed at the end-effector [14]

$$\boldsymbol{M}_{g,i}\dot{\boldsymbol{v}}_{g,i} = \boldsymbol{u}_{g,i} - \boldsymbol{h}_{g,i} \tag{1}$$

where $\boldsymbol{v}_{g,i} = \begin{bmatrix}\dot{\boldsymbol{p}}_{g,i}^{\mathrm{T}} & \boldsymbol{\omega}_{g,i}^{\mathrm{T}}\end{bmatrix}^{\mathrm{T}} \in \mathbb{R}^6$ is the end-effector velocity composed of a linear and an angular component, $\boldsymbol{M}_{g,i} \in \mathbb{R}^{6\times6}$ is the imposed inertia matrix, $\boldsymbol{u}_{g,i} \in \mathbb{R}^6$ is the virtual control input and $\boldsymbol{h}_{g,i} = \begin{bmatrix}\boldsymbol{f}_{g,i}^{\mathrm{T}} & \boldsymbol{\tau}_{g,i}^{\mathrm{T}}\end{bmatrix}^{\mathrm{T}} \in \mathbb{R}^6$ is the wrench exerted by the i manipulator on the object composed of a force and a torque component.

B. Aerial vehicles' dynamics

Concerning the ith quadrotor, the following assumption is made.

Assumption 2. *Without loss of generality and as done in most of the cited works, it is assumed that the cable is attached at the quadrotor's center of mass.*

Because of the above assumption, it is straightforward to see that in the case of taut cable

$$\boldsymbol{p}_{a,i} = \boldsymbol{p}_o - \boldsymbol{R}_o\boldsymbol{r}_{a,i}^o + l_i\boldsymbol{c}_{a,i} \tag{2}$$

where $\boldsymbol{r}_{a,i}^o = \boldsymbol{R}_o^{\mathrm{T}}\boldsymbol{r}_{a,i}$ represents the vector $\boldsymbol{r}_{a,i}$ expressed in the object reference frame Σ_o. The same assumption leads to the following UAV dynamics

$$m_{a,i}\ddot{\boldsymbol{p}}_{a,i} - m_{a,i}\boldsymbol{g} = \boldsymbol{R}_{a,i}\boldsymbol{z}f_{a,i} - t_i\boldsymbol{c}_{a,i} \tag{3}$$

$$\boldsymbol{I}_{a,i}\dot{\boldsymbol{w}}_{a,i} + \boldsymbol{S}(\boldsymbol{w}_{a,i})\boldsymbol{I}_{a,i}\boldsymbol{w}_{a,i} = \boldsymbol{\tau}_{a,i} \tag{4}$$

where $m_{a,i}$ is the mass, $\boldsymbol{g} \in \mathbb{R}^3$ is the gravity vector pointing downwards, $\boldsymbol{I}_{a,i} \in \mathbb{R}^{3\times3}$ is the inertia tensor with respect to the world reference frame Σ_w, t_i is the tension along the ith cable, $f_{a,i} \geq 0$ is the overall force input along axis $\boldsymbol{z} = [0\,0\,1]^{\mathrm{T}}$ in the local reference frame $\Sigma_{a,i}$, $\boldsymbol{S}(\cdot) \in \mathbb{R}^{3\times3}$ is the skew-symmetric matrix built from its vector argument, $\boldsymbol{w}_{a,i}$ is the angular velocity in the frame Σ_w, and $\boldsymbol{\tau}_{a,i}$ is the overall input torque due to thrusters. The dynamics in (3) and (4) can also be expressed in compact form as

$$\boldsymbol{M}_{a,i}\dot{\boldsymbol{v}}_{a,i} + \boldsymbol{n}_{a,i} = \boldsymbol{B}_{a,i}\boldsymbol{u}_{a,i} - \boldsymbol{G}_c\boldsymbol{f}_{c,i}, \tag{5}$$

where

$$\begin{aligned}
\boldsymbol{v}_{a,i} &= \begin{bmatrix}\dot{\boldsymbol{p}}_{a,i}^{\mathrm{T}} & \boldsymbol{\omega}_{a,i}^{\mathrm{T}}\end{bmatrix}^{\mathrm{T}} \in \mathbb{R}^6 \\
\boldsymbol{M}_{a,i} &= \begin{bmatrix}m_{a,i}\boldsymbol{I}_3 & \boldsymbol{O}_3 \\ \boldsymbol{O}_3 & \boldsymbol{I}_{a,i}\end{bmatrix} \in \mathbb{R}^{6\times6} \\
\boldsymbol{n}_{a,i} &= \begin{bmatrix}-m_{a,i}\boldsymbol{g}_{a,i} \\ \boldsymbol{S}(\boldsymbol{w}_{a,i})\boldsymbol{I}_{a,i}\boldsymbol{w}_{a,i}\end{bmatrix} \in \mathbb{R}^6 \\
\boldsymbol{B}_{a,i} &= \begin{bmatrix}\boldsymbol{R}_{a,i}\boldsymbol{z} & \boldsymbol{O}_3 \\ \boldsymbol{0}_3 & \boldsymbol{I}_3\end{bmatrix} \in \mathbb{R}^{6\times4} \\
\boldsymbol{u}_{a,i} &= \begin{bmatrix}f_{a,i} & \boldsymbol{\tau}_{a,i}^{\mathrm{T}}\end{bmatrix}^{\mathrm{T}} \in \mathbb{R}^4 \\
\boldsymbol{G}_c &= \begin{bmatrix}\boldsymbol{I}_3 \\ \boldsymbol{O}_3\end{bmatrix} \in \mathbb{R}^{6\times3} \\
\boldsymbol{f}_{c,i} &= t_i\boldsymbol{c}_{a,i} \in \mathbb{R}^3 \text{ if } t_i \geq 0 \\
\boldsymbol{h}_{c,i} &= \begin{bmatrix}\boldsymbol{f}_{c,i}^{\mathrm{T}} & \boldsymbol{0}_3^{\mathrm{T}}\end{bmatrix}^{\mathrm{T}} \in \mathbb{R}^6
\end{aligned} \tag{6}$$

being $\boldsymbol{I}_n$ the identity matrix in $\mathbb{R}^{n\times n}$, $\boldsymbol{O}_{n\times m}$ the zero matrix in $\mathbb{R}^{n\times m}$ ($\boldsymbol{O}_n$ if $n = m$) and $\boldsymbol{0}_m$ the column vector in $\mathbb{R}^m$ with elements all equal to zero. It is worth remarking that $\boldsymbol{f}_{c,i} = \boldsymbol{0}_3$ in the case the cable is not taut. For the sake of the notation compactness, let us introduce matrix $\boldsymbol{C}_a \in \mathbb{R}^{3N_a\times N_a}$ and the stacked vectors $\boldsymbol{c}_a \in \mathbb{R}^{3N_a}$, $\boldsymbol{t} \in \mathbb{R}^{N_a}$ and $\boldsymbol{f}_c \in \mathbb{R}^{3N_a}$ defined as

$$\begin{aligned}\boldsymbol{C}_a &= \begin{bmatrix} \boldsymbol{c}_{a,1} & \boldsymbol{0}_3 & \dots & \boldsymbol{0}_3 \\ \boldsymbol{0}_3 & \boldsymbol{c}_{a,2} & \dots & \boldsymbol{0}_3 \\ \vdots & \vdots & \ddots & \vdots \\ \boldsymbol{0}_3 & \boldsymbol{0}_3 & \dots & \boldsymbol{c}_{a,N_a} \end{bmatrix} \\ \boldsymbol{c}_a &= \begin{bmatrix} \boldsymbol{c}_{a,1} & \dots & \boldsymbol{c}_{a,N_a} \end{bmatrix}^{\mathrm{T}} \\ \boldsymbol{t} &= \begin{bmatrix} t_1 & \dots & t_{N_a} \end{bmatrix}^{\mathrm{T}} \\ \boldsymbol{f}_c &= \begin{bmatrix} \boldsymbol{f}_{c,1}^{\mathrm{T}} & \dots & \boldsymbol{f}_{c,N_a}^{\mathrm{T}} \end{bmatrix}^{\mathrm{T}}\end{aligned}$$

then, it easily follows that

$$\boldsymbol{f}_c = \boldsymbol{C}_a \boldsymbol{t}, \tag{7}$$

and that

$$\boldsymbol{t} = \boldsymbol{C}_a^{\mathrm{T}} \boldsymbol{f}_c. \tag{8}$$

C. Object dynamics

With regards the object's dynamics, it holds:

$$\begin{aligned} m_o \ddot{\boldsymbol{p}}_o - m_o \boldsymbol{g} &= \boldsymbol{f}_o \\ \boldsymbol{I}_o \dot{\boldsymbol{\omega}}_o + \boldsymbol{S}(\boldsymbol{\omega}_o)\boldsymbol{I}_o \boldsymbol{\omega}_o &= \boldsymbol{\tau}_o \end{aligned} \tag{9}$$

where m_o is the mass of the object, $\boldsymbol{I}_o \in \mathbb{R}^{3\times 3}$ is its inertia tensor in the world reference frame, and $\boldsymbol{\omega}_o$, $\boldsymbol{f}_o$ and $\boldsymbol{\tau}_o$ are, respectively, its angular velocity, the total force and torque acting on it, all expressed in the world frame.

As done in the case of the UAVs, the object dynamics in (9) can also be expressed in compact form

$$\boldsymbol{M}_o \dot{\boldsymbol{v}}_o + \boldsymbol{n}_o = \boldsymbol{h}_o, \tag{10}$$

where

$$\begin{aligned} \boldsymbol{M}_o &= \begin{bmatrix} m_o \boldsymbol{I}_3 & \boldsymbol{O}_3 \\ \boldsymbol{O}_3 & \boldsymbol{I}_o \end{bmatrix} \in \mathbb{R}^{6\times 6} \\ \boldsymbol{v}_o &= \begin{bmatrix} \dot{\boldsymbol{p}}_o^{\mathrm{T}} & \boldsymbol{\omega}_o^{\mathrm{T}} \end{bmatrix}^{\mathrm{T}} \in \mathbb{R}^6 \\ \boldsymbol{n}_o &= \begin{bmatrix} -m_o \boldsymbol{g} \\ \boldsymbol{S}(\boldsymbol{\omega}_o)\boldsymbol{I}_o \boldsymbol{\omega}_o \end{bmatrix} \in \mathbb{R}^6 \\ \boldsymbol{h}_o &= \begin{bmatrix} \boldsymbol{f}_o^{\mathrm{T}} & \boldsymbol{\tau}_o^{\mathrm{T}} \end{bmatrix}^{\mathrm{T}} \in \mathbb{R}^6. \end{aligned} \tag{11}$$

Concerning the total wrench $\boldsymbol{h}_o$ acting on the object, it can be expressed as the sum of the wrench $\boldsymbol{h}_{o,a} = [\boldsymbol{f}_{o,a}^{\mathrm{T}}\, \boldsymbol{\tau}_{o,a}^{\mathrm{T}}]^{\mathrm{T}}$ due to UAVs through cables and the wrench $\boldsymbol{h}_{o,g} = [\boldsymbol{f}_{o,g}^{\mathrm{T}}\, \boldsymbol{\tau}_{o,g}^{\mathrm{T}}]$ due to UGVs

$$\begin{aligned} \boldsymbol{h}_o = \boldsymbol{h}_{o,a} + \boldsymbol{h}_{o,g} &= \sum_{i=1}^{N_a} \boldsymbol{G}(\boldsymbol{r}_{a,i})\boldsymbol{G}_c \boldsymbol{f}_{c,i} + \sum_{i=1}^{N_g} \boldsymbol{G}(\boldsymbol{r}_{g,i})\boldsymbol{h}_{g,i} \\ &= \begin{bmatrix} \bar{\boldsymbol{G}}_a(\boldsymbol{I}_{N_a} \otimes \boldsymbol{G}_c) & \bar{\boldsymbol{G}}_g \end{bmatrix} \begin{bmatrix} \boldsymbol{f}_c \\ \boldsymbol{h}_g \end{bmatrix} \end{aligned} \tag{12}$$

where $\otimes$ denote the Kronecker product operator, $\boldsymbol{G}(\boldsymbol{r}) \in \mathbb{R}^{6\times 6}$is the grasp matrix

$$\boldsymbol{G}(\boldsymbol{r}) = \begin{bmatrix} \boldsymbol{I}_3 & \boldsymbol{O}_3 \\ -\boldsymbol{S}(\boldsymbol{r}) & \boldsymbol{I}_3 \end{bmatrix} \in \mathbb{R}^{6\times 6} \quad \forall\, \boldsymbol{r} \in \mathbb{R}^3 \tag{13}$$

$\boldsymbol{h}_g = [\boldsymbol{h}_{g,1}^T \dots \boldsymbol{h}_{g,N_g}^T]^T \in \mathbb{R}^{6N_g}$ is the stacked vector of forces and wrenches exerted by the ground vehicles at the end-effector contact points, $\bar{\boldsymbol{G}}_a = [\boldsymbol{G}(\boldsymbol{r}_{a,1}) \;\; \cdots \;\; \boldsymbol{G}(\boldsymbol{r}_{a,N_a})] \in \mathbb{R}^{6\times 6N_a}$ and $\bar{\boldsymbol{G}}_g = [\boldsymbol{G}(\boldsymbol{r}_{g,1}) \;\; \cdots \;\; \boldsymbol{G}(\boldsymbol{r}_{g,N_g})] \in \mathbb{R}^{6\times 6N_g}$.

D. Cable feasible wrench analysis

Let us assume that $\underline{t}_i, \overline{t}_i \in \mathbb{R}_0^+$ are respectively the minimum and maximum allowed tensions on the ith cable. The set $\mathcal{D} \in \mathbb{R}^6$ of wrenches $\boldsymbol{h}_{o,a}$ applicable by UAVs to the object is only a proper subset of $\mathbb{R}^6$ (i.e., $\mathcal{D} \subset \mathbb{R}^6$); in fact, in virtue of (12), it is

$$\boldsymbol{h}_{o,a} = \sum_{i=1}^{N_a} \boldsymbol{G}(\boldsymbol{r}_{a,i})\boldsymbol{G}_c \boldsymbol{f}_{c,i} = \sum_{i=1}^{N_a} \begin{bmatrix} \boldsymbol{c}_{a,i} \\ -\boldsymbol{S}(\boldsymbol{R}_o \boldsymbol{r}_{a,i}^o)\boldsymbol{c}_{a,i} \end{bmatrix} t_i = \sum_{i=1}^{N_a} \boldsymbol{\gamma}_i(\boldsymbol{c}_{a,i}) t_i \tag{14}$$

and, then, the set $\mathcal{D}$ is defined as

$$\mathcal{D} = \{\, \boldsymbol{h}_{o,a} \in \mathbb{R}^6 \,|\, \boldsymbol{h}_{o,a} = \sum_{i=1}^{N_a} \boldsymbol{\gamma}_i(\boldsymbol{c}_{a,i}) t_i, 0 \le \underline{t}_i \le t_i \le \overline{t}_i \}. \tag{15}$$

Therefore, a given wrench $\boldsymbol{h}_{o,a}$ is said feasible if it belongs to the zonotope defined by $\mathcal{D}$ [15]. The following lemma holds.

Lemma 1. *Sufficient and necessary conditions to have the UAVs generate any wrench $\boldsymbol{h}_{o,a} \in I\!R^6$ are that $N_a \ge 7$ and that $\sum_{i=1}^{N_a} \boldsymbol{\gamma}_i(\boldsymbol{c}_{a,i}) t_i = \boldsymbol{0}_6$ with t_i having all the same sign.*

Proof. The proof exploits the so called *force closure condition* and is reported in [16]. □

The previous lemma points out the importance of the presented UAV-UGV cooperative framework. In fact, beside the limitation on the maximum value of the tension along cables, the condition $N_a \ge 7$ could be difficult to realize from a practical standpoint; the same applies for the second condition, since an insight into its expression reveals that it requires the UAVs not to be on a single side of the object (see Figure 1).

Remark 1. *Equation* (14) *shows the obvious, yet important, aspect that the set $\mathcal{D}$ depends on both the bounds on the tension t_i and the orientation $\boldsymbol{c}_{a,i}$ of the cable; consequently, the configuration of the aerial vehicles heavily affects the set $\mathcal{D}$ and the admissible wrench distributions among UAVs and UGVs.*

E. Overall system modelling

In this section the overall model of the system depicted in Figure 1 is provided. By taking into consideration (1), (5) and (10), this model can be written as

$$\begin{cases} \boldsymbol{M}_a \dot{\boldsymbol{v}}_a + \boldsymbol{n}_a = \boldsymbol{B}_a \boldsymbol{u}_a - \boldsymbol{h}_c \\ \boldsymbol{M}_g \dot{\boldsymbol{v}}_g = \boldsymbol{u}_g - \boldsymbol{h}_g \\ \boldsymbol{M}_o \dot{\boldsymbol{v}}_o + \boldsymbol{n}_o = \boldsymbol{h}_o \end{cases} \tag{16}$$

with

$$\begin{aligned}
&\boldsymbol{v}_a = \begin{bmatrix}\boldsymbol{v}_{a,1}^{\mathrm{T}} & \dots & \boldsymbol{v}_{a,N_a}^{\mathrm{T}}\end{bmatrix}^{\mathrm{T}},\ \boldsymbol{v}_g = \begin{bmatrix}\boldsymbol{v}_{g,1}^{\mathrm{T}} & \dots & \boldsymbol{v}_{g,N_g}^{\mathrm{T}}\end{bmatrix}^{\mathrm{T}}\\
&\boldsymbol{M}_a = \mathrm{diag}\{\boldsymbol{M}_{a,1}, \dots, \boldsymbol{M}_{a,N_a}\}\\
&\boldsymbol{M}_g = \mathrm{diag}\{\boldsymbol{M}_{g,1}, \dots, \boldsymbol{M}_{g,N_g}\}\\
&\boldsymbol{u}_a = \begin{bmatrix}\boldsymbol{u}_{a,1}^{\mathrm{T}} & \dots & \boldsymbol{u}_{a,N_a}^{\mathrm{T}}\end{bmatrix}^{\mathrm{T}},\ \boldsymbol{u}_g = \begin{bmatrix}\boldsymbol{u}_{g,1}^{\mathrm{T}} & \dots & \boldsymbol{u}_{g,N_g}^{\mathrm{T}}\end{bmatrix}^{\mathrm{T}}\\
&\boldsymbol{h}_c = \begin{bmatrix}\boldsymbol{h}_{c,1}^{\mathrm{T}} & \dots & \boldsymbol{h}_{c,N_a}^{\mathrm{T}}\end{bmatrix}^{\mathrm{T}} = (\boldsymbol{I}_{N_a} \otimes \boldsymbol{G}_c)\boldsymbol{f}_c\\
&\boldsymbol{B}_a = \mathrm{diag}\{\boldsymbol{B}_{a,1}, \dots, \boldsymbol{B}_{a,N_a}\}\\
&\boldsymbol{n}_a = \begin{bmatrix}\boldsymbol{n}_{a,1}^{\mathrm{T}} & \dots & \boldsymbol{n}_{a,N_a}^{\mathrm{T}}\end{bmatrix}^{\mathrm{T}}.
\end{aligned}$$

The model in (16) can be further expressed as

$$\boldsymbol{M}\dot{\boldsymbol{v}} + \boldsymbol{n} = \boldsymbol{B}\boldsymbol{u} - \boldsymbol{h} \tag{17}$$

with

$$\begin{aligned}
\boldsymbol{v} &= \begin{bmatrix}\boldsymbol{v}_a^{\mathrm{T}} & \boldsymbol{v}_g^{\mathrm{T}} & \boldsymbol{v}_o^{\mathrm{T}}\end{bmatrix}^{\mathrm{T}}\\
\boldsymbol{M} &= \mathrm{diag}\{\boldsymbol{M}_a,\ \boldsymbol{M}_g,\ \boldsymbol{M}_o\}\\
\boldsymbol{n} &= \begin{bmatrix}\boldsymbol{n}_a^{\mathrm{T}} & \boldsymbol{0}_{6N_g}^{\mathrm{T}} & \boldsymbol{n}_o^{\mathrm{T}}\end{bmatrix}^{\mathrm{T}}\\
\boldsymbol{u} &= \begin{bmatrix}\boldsymbol{u}_a^{\mathrm{T}} & \boldsymbol{u}_g^{\mathrm{T}}\end{bmatrix}^{\mathrm{T}}\\
\boldsymbol{B} &= \begin{bmatrix}\boldsymbol{B}_a & \boldsymbol{O}_{6N_a \times 6N_g}\\ \boldsymbol{O}_{6N_g \times 4N_a} & \boldsymbol{I}_{6N_g}\\ \boldsymbol{O}_{6\times 4N_a} & \boldsymbol{O}_{6\times 6N_g}\end{bmatrix}\\
\boldsymbol{h} &= \begin{bmatrix}\boldsymbol{h}_c^{\mathrm{T}} & \boldsymbol{h}_g^{\mathrm{T}} & -\boldsymbol{h}_o^{\mathrm{T}}\end{bmatrix}^{\mathrm{T}}
\end{aligned} \tag{18}$$

where $\boldsymbol{h}$, in particular, represents the vector of the constraint wrenches.

From Figure 1 and in the case of taut cables, it is easy to recognize that the model (17) is subject to $6N_g + N_a$ geometrical constraints defined as

$$\begin{cases}
(\boldsymbol{p}_o - \boldsymbol{R}_o\boldsymbol{r}_{a,i}^o - \boldsymbol{p}_{a,i})^{\mathrm{T}}(\boldsymbol{p}_o - \boldsymbol{R}_o\boldsymbol{r}_{a,i}^o - \boldsymbol{p}_{a,i}) = l_i^2,\ \forall\, i\\
\boldsymbol{p}_o - \boldsymbol{p}_{g,i} = \boldsymbol{r}_{g,i},\ \forall\, i\\
\boldsymbol{R}_o^{\mathrm{T}}\boldsymbol{R}_{g,i} = \boldsymbol{R}_{g,i}^o = const,\ \forall\, i
\end{cases} \tag{19}$$

where $\boldsymbol{R}_{g,i}^o$ is the rotation matrix expressing the orientation of frame $\Sigma_{g,i}$ with respect to frame Σ_o and that is constant in the considered case of rigid grasping of a rigid object.

In order to find an expression of the constraint wrenches $\boldsymbol{h}$ to be used in the problem setting in Section II-F, the following lemma is considered.

Lemma 2. *By differentiating twice the constraints in* (19)*, the following relationship is obtained*

$$\boldsymbol{A}_c\dot{\boldsymbol{v}} = \boldsymbol{b}_c \tag{20}$$

where matrix $\boldsymbol{A}_c \in I\!R^{(6N_g+N_a)\times 6(N_a+N_g+1)}$ *and vector* $\boldsymbol{b}_c \in I\!R^{(6N_g+N_a)}$ *depend on both the pose and velocity of the UAVs and UGVs (i.e., on the state of the system).*

Proof. The proof is provided in the Appendix. □

The importance of the previous lemma lies in the fact that it makes possible to apply the Udwadia-Kalaba equation of motion for constrained systems [17]. According to this formulation, the expression of the vector $\boldsymbol{h}$ in (17) is

$$\boldsymbol{h} = -\boldsymbol{M}^{1/2}\left(\boldsymbol{A}_c\boldsymbol{M}^{-1/2}\right)^{\dagger}\left(\boldsymbol{b}_c - \boldsymbol{A}_c\boldsymbol{M}^{-1}(\boldsymbol{B}\boldsymbol{u} - \boldsymbol{n})\right) \tag{21}$$

that relates the constraint wrenches to the system state and to the input $\boldsymbol{u}$. According to the expression of $\boldsymbol{h}$ in (18), the first $6N_a$ elements provide the expression of the constraint wrenches due to cables, i.e., $\boldsymbol{h}_c = (\boldsymbol{I}_{N_a} \otimes \boldsymbol{G}_c)\boldsymbol{f}_c$.

Based on this consideration, let us introduce a selection matrix $\boldsymbol{\Gamma}_a$

$$\boldsymbol{\Gamma}_a = [\boldsymbol{I}_{6N_a} \quad \boldsymbol{O}_{6N_a\times 6N_g+6}]$$

that, based on (18) and (21), allows to find a closed form for the stacked vector $\boldsymbol{h}_c$

$$\begin{aligned}
\boldsymbol{h}_c = \boldsymbol{\Gamma}_a\boldsymbol{h} &= -\boldsymbol{\Gamma}_a\boldsymbol{M}^{1/2}\left(\boldsymbol{A}_c\boldsymbol{M}^{-1/2}\right)^{\dagger}(\boldsymbol{b}_c - \boldsymbol{A}_c\boldsymbol{M}^{-1}(\boldsymbol{B}\boldsymbol{u} - \boldsymbol{n}))\\
&= \boldsymbol{\theta}_c - \boldsymbol{\Theta}_c\boldsymbol{u}
\end{aligned} \tag{22}$$

where

$$\begin{aligned}
\boldsymbol{\theta}_c &= -\boldsymbol{\Gamma}_a\boldsymbol{M}^{1/2}\left(\boldsymbol{A}_c\boldsymbol{M}^{-1/2}\right)^{\dagger}\left(\boldsymbol{b}_c + \boldsymbol{A}_c\boldsymbol{M}^{-1}\boldsymbol{n}\right)\\
\boldsymbol{\Theta}_c &= -\boldsymbol{\Gamma}_a\boldsymbol{M}^{1/2}\left(\boldsymbol{A}_c\boldsymbol{M}^{-1/2}\right)^{\dagger}\boldsymbol{A}_c\boldsymbol{M}^{-1}\boldsymbol{B}
\end{aligned} \tag{23}$$

and that, in turn, together with (8) and the expression of $\boldsymbol{G}_c$ in (6), leads to the following expression of the tension vector $\boldsymbol{t}$:

$$\boldsymbol{t} = \boldsymbol{C}_a^{\mathrm{T}}(\boldsymbol{I}_{N_a}\otimes\boldsymbol{G}_c)^{\mathrm{T}}\boldsymbol{h}_c = \boldsymbol{C}_a^{\mathrm{T}}(\boldsymbol{I}_{N_a}\otimes\boldsymbol{G}_c)^{\mathrm{T}}(\boldsymbol{\theta}_c - \boldsymbol{\Theta}_c\boldsymbol{u}). \tag{24}$$

Moreover, concerning to the total wrench $\boldsymbol{h}_{o,a}$ exerted by the aerial vehicles on the object, it is

$$\boldsymbol{h}_{o,a} = \overline{\boldsymbol{G}}_a\boldsymbol{\Gamma}_a\boldsymbol{h} = \overline{\boldsymbol{G}}_a(\boldsymbol{\theta}_c - \boldsymbol{\Theta}_c\boldsymbol{u}) \tag{25}$$

where (12) and (22) were exploited.

In the same way, let us introduce a selection matrix $\boldsymbol{\Gamma}_g$

$$\boldsymbol{\Gamma}_g = [\boldsymbol{O}_{6N_g\times 6N_a} \quad \boldsymbol{I}_{6N_g} \quad \boldsymbol{O}_{6N_g\times 6}]$$

that, based on (12) and (21), allows to find a closed form for the stacked vector $\boldsymbol{h}_g$

$$\begin{aligned}
\boldsymbol{h}_g = \boldsymbol{\Gamma}_g\boldsymbol{h} &= -\boldsymbol{\Gamma}_g\boldsymbol{M}^{1/2}\left(\boldsymbol{A}_c\boldsymbol{M}^{-1/2}\right)^{\dagger}(\boldsymbol{b}_c - \boldsymbol{A}_c\boldsymbol{M}^{-1}(\boldsymbol{B}\boldsymbol{u} - \boldsymbol{n}))\\
&= \boldsymbol{\theta}_g - \boldsymbol{\Theta}_g\boldsymbol{u}
\end{aligned} \tag{26}$$

where

$$\begin{aligned}
\boldsymbol{\theta}_g &= -\boldsymbol{\Gamma}_g\boldsymbol{M}^{1/2}\left(\boldsymbol{A}_c\boldsymbol{M}^{-1/2}\right)^{\dagger}\left(\boldsymbol{b}_c + \boldsymbol{A}_c\boldsymbol{M}^{-1}\boldsymbol{n}\right)\\
\boldsymbol{\Theta}_g &= -\boldsymbol{\Gamma}_g\boldsymbol{M}^{1/2}\left(\boldsymbol{A}_c\boldsymbol{M}^{-1/2}\right)^{\dagger}\boldsymbol{A}_c\boldsymbol{M}^{-1}\boldsymbol{B}.
\end{aligned} \tag{27}$$

Finally, the expression of the total wrench exerted by the robots on the object, $\boldsymbol{h}_{o,g}$, directly comes by considering (12) and (26)

$$\boldsymbol{h}_{o,g} = \overline{\boldsymbol{G}}_g\boldsymbol{h}_g = \overline{\boldsymbol{G}}_g(\boldsymbol{\theta}_g - \boldsymbol{\Theta}_g\boldsymbol{u}). \tag{28}$$

F. Problem formulation

We are now ready to state the main problem of the paper. The main idea behind the combination of aerial and ground vehicles is to merge their complementary features: the precision of ground robots and the high payload of multiple tethered aerial vehicles. Therefore, it makes sense that the aerial vehicles are in charge of most of the wrench required to move the object, while the ground robots are in charge of counteracting any source of uncertainty. In this way, the advantages of both the typologies of robots are considered. This idea is formalized in the following problem.

Problem 1. *Let us consider a desired trajectory of the object starting at time t_0 and ending at t_f specified in terms of position $\boldsymbol{p}_{o,d}(t)$ and orientation $\mathbb{R}_{o,d}(t)$ (and corresponding velocity and acceleration $\boldsymbol{v}_{o,d}$, $\dot{\boldsymbol{v}}_{o,d}$). The required wrench $\boldsymbol{h}_{o,d}$ on the object can be computed by inverse dynamics in* (10)*. We seek for the optimal trajectories of the UAVs $\boldsymbol{p}_{a,i}(t)$, $\boldsymbol{R}_{a,i}(t)$, $\forall\, i$, such as to solve the following global optimization problem:*

$$\min_{\boldsymbol{u}_{[t_0,t_f]}} \; J(t_0) = \int_{t_0}^{t_f} l(t)dt$$

with

$$l(t) = \gamma_1 \|\boldsymbol{h}_{o,a} - \boldsymbol{h}_o\|^2 + \gamma_2 \left\| \begin{bmatrix} \boldsymbol{h}_c \\ \boldsymbol{h}_g \end{bmatrix} \right\|^2 + \gamma_3 V(\mathcal{D})^{-1} \tag{29}$$

$$s.t.$$

1) $\boldsymbol{h}_{o,d}(t) = \boldsymbol{h}_{o,a}(t) + \boldsymbol{h}_{o,g}(t)$ *object's wrench constraint*
2) $\boldsymbol{M}\dot{\boldsymbol{v}} + \boldsymbol{n} = \boldsymbol{B}\boldsymbol{u} - \boldsymbol{h}$ *system's dynamics*
3) $\underline{\boldsymbol{t}} \leq \boldsymbol{t} \leq \overline{\boldsymbol{t}}$ *cable tension constraints*
4) $\boldsymbol{c}_{a,i} \in \mathcal{S}(t), \forall\, i$ *cable attitude constraints*
5) $\underline{\boldsymbol{u}} \leq \boldsymbol{u} \leq \overline{\boldsymbol{u}}$ *input constraints*

where γ_r $(r = 1, 2, 3)$ are positive scalar weights, $\boldsymbol{u}_{[t_0,t_f]}$ is the control input in the interval $[t_0,\, t_f]$, $V(\mathcal{D})$ is the volume of the polytope $\mathcal{D}$ defined in (15), $\underline{\boldsymbol{t}}$ ($\overline{\boldsymbol{t}}$) is a vector whose ith element is $\underline{t}_i$ ($\overline{t}_i$), $\underline{\boldsymbol{u}}$ ($\overline{\boldsymbol{u}}$) represents the lower (upper) bound for the control input $\boldsymbol{u}$, and $\mathcal{S}(t)$ is the set constraining the cables' attitude to account, for example, for requirements on the minimum distance between vehicles or to keep the UAVs always above the object. The $\leq$ operator in 3) and 5) is to be intended element-wise.

The ratio behind $l(t)$ is that the first term tries to have the overall load carried by the UAVs and the second term avoids that such a choice results in a too inefficient solution concerning the overall forces along the UAVs' cables and at the UGVs' end-effectors. The last term accounts for the volume of the zonotope $\mathcal{D}$ defined in Section II-D: the greater this volume the larger the set of the applicable wrenches by the UAVs. The effects of this term will be also highlighted in Section IV.

From (22) and (26), $l(t)$ can be rewritten as

$$\begin{aligned} l(t) &= \gamma_1 \|\boldsymbol{h}_{o,a} - \boldsymbol{h}_o\|^2 + \gamma_2 \left\| \begin{bmatrix} \boldsymbol{h}_c \\ \boldsymbol{h}_g \end{bmatrix} \right\|^2 + \gamma_3 V(\mathcal{D})^{-1} \\ &= \gamma_1 \|\overline{\boldsymbol{G}}_a(\boldsymbol{\theta}_c - \boldsymbol{\Theta}_c \boldsymbol{u}) - \boldsymbol{h}_o\|^2 + \gamma_2 \left\| \begin{bmatrix} \boldsymbol{\theta}_c \\ \boldsymbol{\theta}_g \end{bmatrix} - \begin{bmatrix} \boldsymbol{\Theta}_c \\ \boldsymbol{\Theta}_g \end{bmatrix} \boldsymbol{u} \right\|^2 \\ &\quad + \gamma_3 V(\mathcal{D})^{-1} \end{aligned} \tag{30}$$

Remark 2. *Thanks to the modeling of the system made in Section II, the local performance index $l(t)$ is expressed in* (30) *as a non-linear function of the control input $\boldsymbol{u}$ and of the overall state of the system composed by the position and the orientation of both the UAVs and the UGV end-effectors (and their first derivatives). In particular, the state affects the volume $V(\mathcal{D})$, vectors $\boldsymbol{\theta}_c$, $\boldsymbol{\theta}_g$ and matrices $\boldsymbol{\Theta}_c$, $\boldsymbol{\Theta}_g$.*

III. Problem solution

The complexity of the performance index function and the type and number of constraints make it difficult or impossible to analytically solve Problem 1. Dynamic Programming (DP) represents a powerful tool for solving such kind of problems regardless how much complex they are, but it has as major drawback the computational effort required to obtain numerical solutions in the case of continuous-state space problems. In this case, the state-space needs to be discretized, and the accuracy of the solution depends on the adopted mesh. As further issue, because of the state and the control input discretization, the resolution procedure often requires interpolation of the performance index at points not belonging to the mesh [18]. Furthermore, DP also suffers of "curse of dimensionality" with regards to the dimension of the state and control input spaces. In our case, since the position of the object is assigned, the manipulators rigidly grasp the object and the cables are taut, the configuration of the overall system exclusively depends on the state vector of the cable directions $\boldsymbol{c}_a(t)$ and on its derivative $\dot{\boldsymbol{c}}_a(t)$.

Remark 3. *Actually, also the orientation of the UAVs should be considered to describe the overall configuration of the system. However, it is well known that the model in* (5) *is differentially flat with respect to the couple $(\boldsymbol{p}_{a,i},\, \psi_{a,i})$ where $\psi_{a,i}$ is the yaw angle of the quadrotor. This means that the overall orientation of the UAVs can be computed from the knowledge of the position $\boldsymbol{p}_{a,i}$, that can be computed starting from $\boldsymbol{c}_{a,i}$, and $\psi_{a,i}$ that is here set to zero [19].*

The Problem 1 is formulated in its discrete form as

$$\min_{\boldsymbol{u}_{[k_0,k_f]}} \; J(k_0) = \sum_{k_0}^{k_f} l(k)T \tag{31}$$

1) $\boldsymbol{h}_{o,d}(k) = \boldsymbol{h}_o(k) = \boldsymbol{h}_{o,a}(k) + \boldsymbol{h}_g(k)$
2) $\boldsymbol{v}(k+1) = \boldsymbol{v}(k) + T\boldsymbol{M}^{-1}(k)[\boldsymbol{B}\boldsymbol{u}(k) - \boldsymbol{h} - \boldsymbol{n}]$
3) $\underline{\boldsymbol{t}} \leq \boldsymbol{t} \leq \overline{\boldsymbol{t}}$
4) $\boldsymbol{c}_{a,i}(k) \in \mathcal{S}(k), \forall\, i$
5) $\underline{\boldsymbol{u}} \leq \boldsymbol{u} \leq \overline{\boldsymbol{u}}$

where $l(\cdot)$ has the same expression as in (30), $\boldsymbol{u}_{[k_0,k_f]}$ is the control sequence. Forward Euler method with sample time $T \in \mathbb{R}^+$ has been used to approximate equations of motion, $\cdot(k)$ is the value of the generic function at $t = kT$, and k_0 and k_f are the initial and final step times, respectively. The solution of this problem follows the classical approach consisting in building a grid $\mathcal{G}$ such as each point is represented by $(k, \boldsymbol{s}(k))$ with $\boldsymbol{s}(k) = [\boldsymbol{c}_a(k)^{\mathrm{T}}, \dot{\boldsymbol{c}}_a(k)^{\mathrm{T}}]^{\mathrm{T}}$; obviously, points not meeting the geometrical constraint 4) in (31) are not included. Moreover, the resolution makes use of the Bellman's Principle and is, then, backward from the set of final states to the initial states; indeed, by defining $J^\star(\boldsymbol{s}(k+1), \boldsymbol{u}(k+1))$ as the optimal solution from the state $\boldsymbol{s}(k+1)$ when the optimal input sequence is applied, the optimal input $\boldsymbol{u}(k)$ can be computed by solving the minimization problem

$$J^\star(\boldsymbol{s}(k), \boldsymbol{u}(k)) = \min_{\boldsymbol{u}(k)} \left(l(k) + J^\star(\boldsymbol{s}(k+1), \boldsymbol{u}(k+1)) \right) \tag{32}$$

while meeting the constraints in (31). The above equation makes evident that the approach generally requires to discretize the input space, to evaluate $J(\boldsymbol{s}(k), \boldsymbol{u}(k))$ for all possible $\boldsymbol{u}(k))$ satisfying the constraint 5) and to discard control inputs that not meet this constraints; however, because of the dimension of the control input such an approach might be unfeasible in this case. To overcome this issue, one might exploit the modeling of Section II and analytically solve (32). In detail, at each step k and for each couple $\boldsymbol{s}(k), \boldsymbol{s}(k+1) \in \mathcal{G}$, the input $\boldsymbol{u}(k)$ can be computed by

solving a quadratic programming problem by resorting to standard software as Matlab or CPLEX:

$$\min_{\boldsymbol{u}(k)} l(k)=\gamma_1\|\overline{\boldsymbol{G}}_a(\boldsymbol{\theta}_c-\boldsymbol{\Theta}_c\boldsymbol{u})-\boldsymbol{h}_o\|^2+\gamma_2\left\|\begin{bmatrix}\boldsymbol{\theta}_c\\ \boldsymbol{\theta}_g\end{bmatrix}-\begin{bmatrix}\boldsymbol{\Theta}_c\\ \boldsymbol{\Theta}_g\end{bmatrix}\boldsymbol{u}\right\|^2+\gamma_3 V(\mathcal{D})^{-1}$$

$$s.t. \tag{33}$$

1) $\boldsymbol{h}_{o,d}(k)=\boldsymbol{h}_o(k)=\boldsymbol{h}_{o,a}(k)+\boldsymbol{h}_g(k)$
2) $\boldsymbol{v}(k+1)=\boldsymbol{v}(k)+T\boldsymbol{M}^{-1}(k)[\boldsymbol{B}\boldsymbol{u}(k)-\boldsymbol{h}(k)-\boldsymbol{n}(k))]$
3) $\underline{\boldsymbol{t}}\leq \boldsymbol{C}_a^{\mathrm{T}}(\boldsymbol{I}_{N_a}\otimes\boldsymbol{G}_c)^{\mathrm{T}}(\boldsymbol{\theta}_c-\boldsymbol{\Theta}_c\boldsymbol{u})\leq\overline{\boldsymbol{t}}$
4) $\underline{\boldsymbol{u}}\leq\boldsymbol{u}\leq\overline{\boldsymbol{u}}$

where in constraint 2) the velocity $\boldsymbol{v}(k)$ ($\boldsymbol{v}(k+1)$) can be computed from $\boldsymbol{s}(k)$ ($\boldsymbol{s}(k+1)$), and in constraint 3) equation (24) is exploited. It is easy to recognize that the performance index and the constraints are quadratic and linear functions of $\boldsymbol{u}$, respectively. The need of minimizing over $\boldsymbol{u}(k)$ is motivated by the fact that the transition from $\boldsymbol{s}(k)$ to $\boldsymbol{s}(k+1)$ can either have no solution, and in such case the transition is marked as unfeasible, or even have an infinite number of solutions. The latter case can be intuitively demonstrated by considering that a given wrench on the object and given trajectories of the UAVs and the UGVs can be obtained by different control inputs that generate different internal stresses to the object, i.e., wrenches on the object that not induce any motion on it. The formal proof of such statement is here omitted for the sake of space.

Remark 4. *It is worth remarking that several solutions were presented to apply DP to the case of high state dimension as in [20], [21]. This paper does not aim to further contribute to develop efficient implementation of DP; instead, it aims at using DP as a tool to solve Problem 1 which exploits modeling in Section II.*

IV. Numerical examples

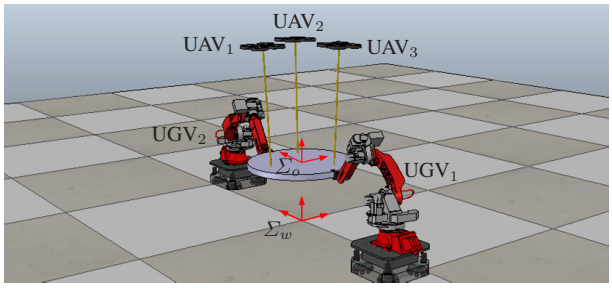

Fig. 2. Simulation setup with $N_a=3$ aerial vehicles (UAV$_i$, $i=1,2,3$) and $N_g=2$ ground robots (UGV$_i$, $i=1,2$).

In this section, simulation results concerning the transport of a load by 3 ($N_a=3$) aerial vehicles and 2 ($N_g=2$) ground vehicles shown in Figure 2 are presented. The ground vehicles are anthropomorphic arms mounted on holonomic mobile bases able to move in $x-y$ plane with imposed inertia matrix $\boldsymbol{M}_{g,i}=\mathrm{diag}\{\boldsymbol{I}_3\mathrm{Kg},\boldsymbol{I}_3\mathrm{Kgm}^2\}$ ($i=1,2$); the aerial vehicles have mass $m_{a,i}=1\,\mathrm{Kg}$, inertia tensor $\boldsymbol{I}_{a,i}^{a,i}=\mathrm{diag}\{0.007,0.007,0.015\}\mathrm{Kgm}^2$ in the frame $\Sigma_{a,i}$ and cable length $l_i=1\,\mathrm{m}$ ($i=1,2,3$). The load to transport is a cylinder with diameter $0.9\,\mathrm{m}$, height $0.05\,\mathrm{m}$, mass $m_o=5\,\mathrm{Kg}$ and tensor of inertia $\boldsymbol{I}_o^o=\mathrm{diag}\{0.25,0.25,0.5\}\,\mathrm{Kgm}^2$ expressed in the frame Σ_o; moreover, it is:

$$\boldsymbol{r}_{a,i}^o=0.3\,[\cos(\alpha_i)\ \ \sin(\alpha_i)\ \ 0]^{\mathrm{T}}\ \mathrm{m},\ \alpha_i=-2\pi(i-1)/3$$
$$\boldsymbol{r}_{g,i}^o=0.45\,[\cos(\alpha_i)\ \ \sin(\alpha_i)\ \ 0]^{\mathrm{T}}\ \mathrm{m},\ \alpha_i=\pi(3-2i)/2.$$

Herein, we reduce the dimension of the state space $\boldsymbol{s}(k)$ defined in Section II-F assuming that $\boldsymbol{c}_{a,i}$, expressed in frame Σ_o, is such as

$$\boldsymbol{c}_{a,i}^o=[-\cos(\theta_i)\sin(\phi(k))\ \ -\sin(\theta_i)\sin(\phi(k))\ \ \cos(\phi(k))]^{\mathrm{T}} \tag{34}$$

with $\theta_i=-2\pi(i-1)/3$; this basically implies that the UAVs are in formation and that this formation is parametrized with respect to the angle $\phi(k)$ (see Figure 1). Therefore, the state $\boldsymbol{s}(k)$ is such as $\boldsymbol{s}(k)=[\phi(k)\ \dot{\phi}(k)]^{\mathrm{T}}$ and a sub-optimal solution is found (see Remark 4).
With regards to the system constraints in (31), the minimum and maximum cable tensions are 2 N and 60 N, respectively, while no constraint is assumed on $\boldsymbol{u}$ for the sake of brevity. Furthermore, it is required that $0.05\leq\phi\leq\pi/2$ in order to avoid collisions between the UAVs and to keep them on top of the object (see Figure 2), while $\dot{\phi}$ is constrained to belong to the range $[-2\ 2]\,\mathrm{rad/s}$ and the sample time in (31) is set to $T=0.05\,\mathrm{s}$.
It is required that the load is lifted from its initial position $[0\ \ 0\ \ 0.5]^{\mathrm{T}}\mathrm{m}$ ($t_0=0\,\mathrm{s}$) to $[0\ \ 0\ \ 1]^{\mathrm{T}}\mathrm{m}$ ($t=1.5\,\mathrm{s}$); then, it makes a movement of $5\,\mathrm{m}$ along the x-axis up to $[5\ \ 0\ \ 1]^{\mathrm{T}}\mathrm{m}$ ($t=11.5\,\mathrm{s}$); in the end, it reaches the final position $[5\ \ 0\ \ 0.5]^{\mathrm{T}}\mathrm{m}$ ($t=13\,\mathrm{s}$). The object orientation is kept constant during the initial phase of the trajectory up to $t=4.5\,\mathrm{s}$; starting from this time, an elementary rotation by $\beta=\pi/6$ about the y-axis of the Σ_w is continuously applied up to $t=7.5\,\mathrm{s}$. The overall trajectory lasts $t_f=13\,\mathrm{s}$ and is shown in Figure 3. Two case studies are presented that differ in the considered objective function, and a video of the simulations can be found at the following link[1].

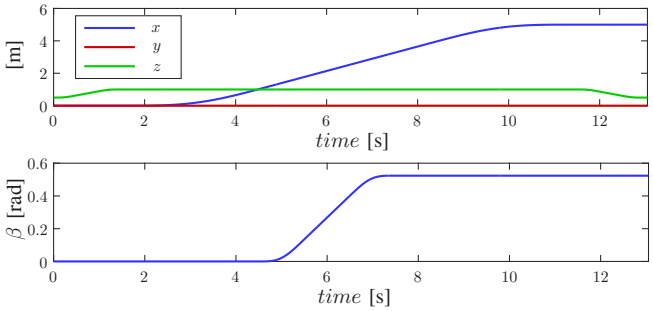

Fig. 3. Desired object trajectory in terms of position (top) and orientation (down).

A. First case study

In the first case study, weights in (29) are selected as $\gamma_1=0.9$, $\gamma_2=0.1$ and $\gamma_3=0$; such choice implies that the term $V(\mathcal{D})$ is not considered in the optimization function. Figure 4 shows at some relevant time steps how the object desired force $\boldsymbol{f}_{o,d}=\boldsymbol{f}_{o,a}+\boldsymbol{f}_{o,g}$ is distributed between aerial and ground vehicles and how, in turn, $\boldsymbol{f}_{o,a}$ and $\boldsymbol{f}_{o,g}$ are distributed among the UAV cables and the ground robots, respectively. For ease of representation, only

[1] www.automatica.unisa.it/video/CoopTranspICRA2018.mp4

forces are reported. Furthermore, Figures 5 and 6 report the time plots of $\phi(t)$ ($\dot{\phi}(t)$) and of the tensions along the cables, respectively. No constraints on the initial and final values of ϕ are set (free boundary condition), while it is set $\dot{\phi}(t_0) = \dot{\phi}(t_f) = 0$; therefore, it is selected the solution that, considering all the possible starting configurations, minimizes the overall performance index J. In this case, it is the one starting from minimum allowed ϕ. During the first lifting motion, when only a vertical force is required, the UAVs tend to get as close as possible to the z-axis of frame Σ_o in order to exert most of the desired force ($\boldsymbol{f}_{o,a} \approx \boldsymbol{f}_{o,d}$ and $\boldsymbol{f}_{o,g} \approx \boldsymbol{0}_3$), while minimizing $\boldsymbol{h}_g$ and $\boldsymbol{h}_c$; moreover, the symmetry of the problem results in equally distributed tensions along the cables in this phase (Figure 6). Intuitively, this is obtained by keeping the cables aligned along the direction of motion. On the contrary, during the first part of the horizontal motion (from $t = 1.5$ s up to $t = 4.5$ s), the angle ϕ increases in order to make the UAVs able to generate forces also along the x-axis (see Section II-D). Figures 4 and 6 show that this is associated to a different tension distribution among the cables and that the tension is higher along $\boldsymbol{c}_{a,2}$ and $\boldsymbol{c}_{a,3}$ and lower along $\boldsymbol{c}_{a,1}$. Instead, when the orientation is required to change (from $t = 4.5$ s to $t = 7.5$s), the angle ϕ tends to reduce to align the cables to the z-axis of frame Σ_o and, simultaneously, the tension increases along $\boldsymbol{c}_{a,1}$ and decreases along the other two cables; this is in order to efficiently rotate the load. After the orientation has been completed and during the last portion of the horizontal motion (from $t = 7.5$ s up to $t = 11.5$ s), the formation keeps almost constant and the first cable (whose direction is almost vertical) is in charge of providing most of the contribution to compensate the object gravity, while the other cables are in charge of the horizontal motion.

In the end, during the last vertical motion from $t = 11.5$ s to $t = 13$ s, the formation keeps almost constant with large value of the angle ϕ, while tensions are time-varying and greater along $\boldsymbol{c}_{a,1}$. In such configuration, one would expect to have the cables aligned with the z-axis of frame Σ_w; however, the parametrization of the formation through the angle ϕ does not allow this configuration. Finally, for the sake of space, the control input $\boldsymbol{u}(t)$ is not reported.

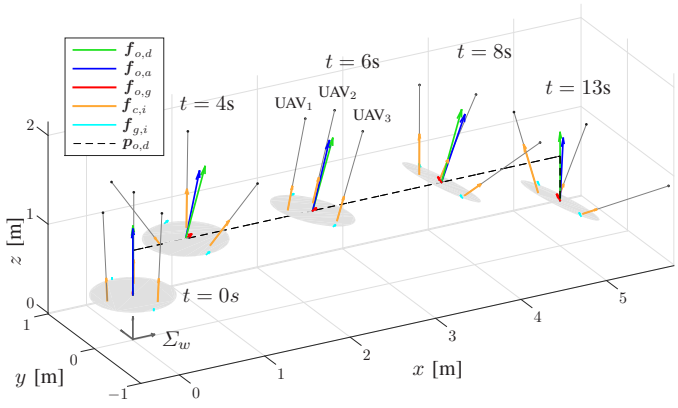

Fig. 4. First case study. System configuration at different time steps. For each of them, the positions of the object and of the UAVs (points in the figure) and the distribution of the desired force $\boldsymbol{f}_{o,d}$ are represented. The vectors in the figure are normalized with respect to the maximum norm of $||\boldsymbol{f}_{o,d}||$ over the interval $[t_0, t_f]$.

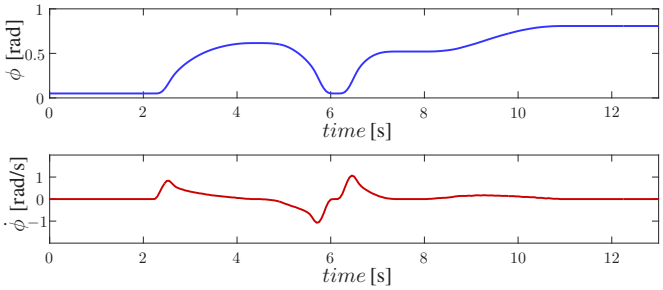

Fig. 5. First case study. Optimal solution of ϕ (top) and $\dot{\phi}$ (bottom).

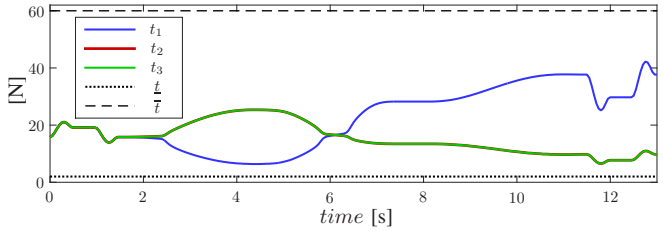

Fig. 6. First case study. Tensions along the cables. Tensions related to UAVs 2 and 3 show the same evolution since they are symmetric with respect to the desired trajectory.

B. Second case study

In the second case study, weights in (29) are chosen as $\gamma_1 = 0.012$, $\gamma_2 = 0.008$ and $\gamma_3 = 0.98$. The difference with respect to the previous case study is that the term $V(\mathcal{D})$ now highly affects the performance index. In detail, from Figures 7 and 8, it follows that the general trend of the optimal solution is preserved but higher values of ϕ (and then of $V(\mathcal{D})$) are obtained. For example, during the first vertical motion, the starting value of ϕ is not equal to its minimum value (i.e., $\phi = 0.05$: cables are almost aligned along the z-axis of frame Σ_o) but it is equal to $\phi = \pi/8$. In this case, the set $\mathcal{D}$ has not zero volume and, then, the UAVs are able to generate forces also along directions other than the vertical one without the UGVs contribution; this feature makes it possible to reject external disturbances along any directions in the execution phase via feedback control.

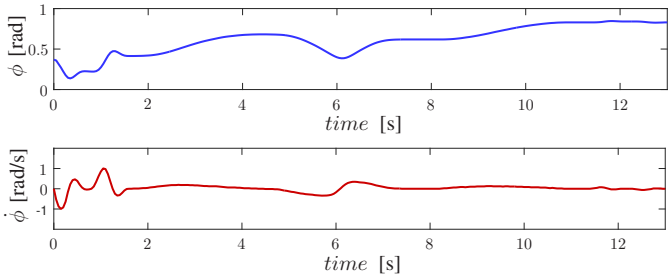

Fig. 7. Second case study. Optimal solution of ϕ (top) and $\dot{\phi}$ (down).

V. Conclusions

The paper aimed to lay the foundation of a framework for the cooperative transportation of a load by a heterogeneous team composed by UAVs and UGVs. UAVs are attached to the load by inextensible cables and are free to float around the cable attachment points on the object. Such a redundancy is exploited together with the system model to set an optimal

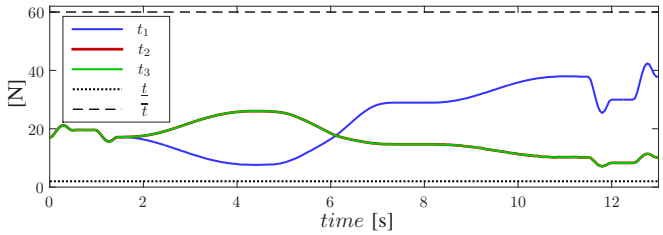

Fig. 8. Second case study. Tensions along the cables.

planning problem that takes into account several objectives, as the load distribution among UAVs and UGVs and the space of feasible wrenches that can be generated by UAVs. Future work will be aimed at designing a decentralized control scheme for such a system and at running experiments on a real platform.

APPENDIX

Proof of Lemma 2

In order to get (20) from (19), the latter must be twice differentiated with respect to time and this second derivative must be linear in the vector $\dot{\boldsymbol{v}}$. In light of this, by considering that $\boldsymbol{r}^o_{g,i} = \boldsymbol{R}_o^{\mathrm{T}} \boldsymbol{r}_{g,i} \, \forall \, i$, the first derivatives of the equations in (19) are computed

$$\begin{cases} (\dot{\boldsymbol{p}}_o - \boldsymbol{S}(\boldsymbol{\omega}_o)\boldsymbol{r}_{a,i} - \dot{\boldsymbol{p}}_{a,i})^{\mathrm{T}}(\boldsymbol{p}_o - \boldsymbol{r}_{a,i} - \boldsymbol{p}_{a,i}) = 0, \, \forall \, i \\ \dot{\boldsymbol{p}}_o - \dot{\boldsymbol{p}}_{g,i} = \boldsymbol{S}(\boldsymbol{\omega}_o)\boldsymbol{r}_{g,i}, \, \forall \, i \\ \boldsymbol{\omega}_{g,i} - \boldsymbol{\omega}_o = \boldsymbol{0}_3, \, \forall \, i. \end{cases} . \tag{35}$$

Then, by differentiating (35), one obtains

$$\begin{cases} (\ddot{\boldsymbol{p}}_o + \boldsymbol{S}(\boldsymbol{r}_{a,i})\dot{\boldsymbol{\omega}}_o - \boldsymbol{S}^2(\boldsymbol{\omega}_o)\boldsymbol{r}_{a,i} - \ddot{\boldsymbol{p}}_{a,i})^{\mathrm{T}}(\boldsymbol{p}_o - \boldsymbol{r}_{a,i} - \boldsymbol{p}_{a,i}) + \\ \quad (\dot{\boldsymbol{p}}_o - \boldsymbol{S}(\boldsymbol{\omega}_o)\boldsymbol{r}_{a,i} - \dot{\boldsymbol{p}}_{a,i})^{\mathrm{T}}(\dot{\boldsymbol{p}}_o - \boldsymbol{S}(\boldsymbol{\omega}_o)\boldsymbol{r}_{a,i} - \dot{\boldsymbol{p}}_{a,i}) = 0, \, \forall \, i \\ \ddot{\boldsymbol{p}}_o - \ddot{\boldsymbol{p}}_{g,i} = -\boldsymbol{S}(\boldsymbol{r}_{g,i})\dot{\boldsymbol{\omega}}_o + \boldsymbol{S}^2(\boldsymbol{\omega}_o)\boldsymbol{r}_{g,i}, \, \forall \, i \\ \dot{\boldsymbol{\omega}}_{g,i} - \dot{\boldsymbol{\omega}}_o = \boldsymbol{0}_3, \, \forall \, i. \end{cases} \tag{36}$$

It is straightforward to verify that the equations in (36) are linear in the components of $\dot{\boldsymbol{v}}$; this proves the lemma. The expression of $\boldsymbol{A}_c$ and $\boldsymbol{b}_c$ are not provided for the sake of space.

REFERENCES

[1] G. Gioioso, A. Franchi, G. Salvietti, S. Scheggi, and D. Prattichizzo. The flying hand: A formation of uavs for cooperative aerial tele-manipulation. In *Proceedings of IEEE International Conference on Robotics and Automation*, pages 4335–4341, 2014.

[2] K. Sreenath and V. Kumar. Dynamics, control and planning for cooperative manipulation of payloads suspended by cables from multiple quadrotor robots. In *Proceedings of Robotics: Science and Systems*, 2013.

[3] M.M. Nicotra, E. Garone, R. Naldi, and L. Marconi. Nested saturation control of an uav carrying a suspended load. In *Proceedings of American Control Conference*, pages 3585–3590, 2014.

[4] K. Sreenath T. Lee and V. Kumar. Geometric control of cooperating multiple quadrotor uavs with a suspended payload. In *IEEE Conference on Decision and Control*, pages 5510–5515, 2013.

[5] C. Masone, H. H. Blthoff, and P. Stegagno. Cooperative transportation of a payload using quadrotors: A reconfigurable cable-driven parallel robot. In *2016 IEEE/RSJ International Conference on Intelligent Robots and Systems (IROS)*, pages 1623–1630, 2016.

[6] T. Lee S. Dai and D. S. Bernstein. Adaptive control of a quadrotor uav transporting a cable-suspended load with unknown mass. In *53rd IEEE Conference on Decision and Control*, pages 6149–6154, 2014.

[7] K. Sreenath, Taeyoung Lee, and V. Kumar. Geometric control and differential flatness of a quadrotor uav with a cable-suspended load. In *Proceeding of IEEE 52nd Annual Conference on Decision and Control*, pages 2269–2274, 2013.

[8] M. Tognon and A. Franchi. Dynamics, control, and estimation for aerial robots tethered by cables or bars. *IEEE Transaction on Robotics*, 33:834–845, 2017.

[9] G. Wu and K. Sreenath. Geometric control of multiple quadrotors transporting a rigid-body load. In *IEEE Conference on Decision and Control*, pages 6141–6148, 2014.

[10] G. Tartaglione, E. DAmato, M. Ariola, P. S. Rossi, and T. A. Johansen. Model predictive control for a multi-body slung-load system. *Robotics and Autonomous Systems*, 92:1–11, 2017.

[11] T. Nguyen and E. Garone. Control of a uav and a ugv cooperating to manipulate an object. In *American Control Conference (ACC)*, pages 1347–1352, 2016.

[12] A. Gasparri R. Naldi and E. Garone. Cooperative pose stabilization of an aerial vehicle through physical interaction with a team of ground robots. In *IEEE International Conference on Control Applications*, pages 415–420, 2012.

[13] N. Staub, M. Mohammadi, D. Bicego, D. Prattichizzo, and A. Franchi. Towards robotic magmas: Multiple aerial-ground manipulator systems. In *IEEE International Conference on Robotics and Automation (ICRA)*, pages 1307–1312, 2017.

[14] O. Khatib. A unified approach for motion and force control of robot manipulators: The operational space formulation. *IEEE Journal on Robotics and Automation*, 3(1):43–53, 1987.

[15] S. Bouchard, C. Gosselin, and B. Moore. On the ability of a cable-driven robot to generate a prescribed set of wrenches. *Journal of Mechanisms and Robotics*, 2(1):1–10, 2010.

[16] H. Kino, T. Yahiro, F. Takemura, and T. Morizono. Robust PD control using adaptive compensation for completely restrained parallel-wire driven robots: Translational systems using the minimum number of wires under zero-gravity condition. *IEEE Transactions on Robotics*, 23(4):803–812, 2007.

[17] F. Udwadia and R. Kalaba. What is the General Form of the Explicit Equations of Motion for Constrained Mechanical Systems? *Journal of Applied Mechanics*, 69(3):335 – 335, 2002.

[18] S. M Lavalle and P. Konkimalla. Algorithms for computing numerical optimal feedback motion strategies. *The International Journal of Robotics Research*, 20(9):729–752, 2001.

[19] S. Formentin and M. Lovera. Flatness-based control of a quadrotor helicopter via feedforward linearization. In *Decision and Control and European Control Conference (CDC-ECC), 2011 50th IEEE Conference on*, pages 6171–6176. IEEE, 2011.

[20] W. B.Powell. *Approximate Dynamic Programming: Solving the curses of dimensionality*, volume 703. John Wiley & Sons, 2007.

[21] P. Elbert, S. Ebbesen, and L. Guzzella. Implementation of dynamic programming for n-dimensional optimal control problems with final state constraints. *IEEE Transactions on Control Systems Technology*, 21(3):924–931, 2013.